Numerical evaluation of droplet sizing based on the ratio of the fluorescent and scattered light intensities (LIF/Mie technique)

Georgios Charalampous,[1,*] and Yannis Hardalupas,[1]

[1]*Mechanical Engineering Department, Imperial College London, Exhibition Rd, London SW7 2AZ, UK*

[*]*Corresponding author:georgios.charalampous@imperial.ac.uk*

The dependence of fluorescent and scattered light intensities from spherical droplets on droplet diameter was evaluated using Mie theory. The emphasis is on the evaluation of droplet sizing, based on the ratio of laser induced fluorescence and scattered light intensities (LIF/Mie technique). A parametric study is presented, which includes the effects of scattering angle, the real part of the refractive index and the dye concentration in the liquid (determining the imaginary part of the refractive index). The assumption that the fluorescent and scattered light intensities are proportional to the volume and surface area of the droplets for accurate sizing measurements is not generally valid. More accurate sizing measurements can be performed with minimal dye concentration in the liquid and by collecting light at a scattering angle of 60° rather than the commonly used angle of 90°. Unfavorable to the sizing accuracy are oscillations of the scattered light intensity with droplet diameter that are profound at the sidescatter direction (90°) and for droplets with refractive indices around 1.4.

OCIS codes: 290.5850, 300.2530, 120.3940, 280.1100

1. Introduction

Sprays are used in many industries where, depending on the application, there are particular demands on the atomization of the sprayed liquid. The combustion of liquid fuels requires fine atomization to promote vaporization, which in turn enhances mixing and combustion efficiency and reduces the production of pollutants. In crop spraying, relatively large drop sizes with narrow spread of the distribution are required to promote gravitationally settling and avoid droplet carry over by air currents and enhance even dispersion over a sprayed field. For drug inhalers, it is essential that very fine droplets are produced that follow the air flow into the lungs to deliver the drug. It is evident that the size of the spray droplets is a key feature of spray characteristics. For this reason, the design and evaluation of sprays requires tools that facilitate quick and accurate measurement of droplet size. Laser based methods have been developed for droplet sizing, since laser probing offers advantages over physical probing, which include non-intrusive measurement, high spatial resolution that can be as fine as the laser wavelength and application in harsh or corrosive environments.

The principles of each laser-based method for droplet sizing vary considerably. The Phase Doppler Anemometer [1-5] or PDA measures the size and velocity of droplets at a ‘point’ determined by a probe volume formed by two crossing laser beams. The laser diffraction technique [6-9] obtains line of sight sizing measurements along the path of a laser beam passing through a spray. The diffraction pattern of the droplets crossing the beam path is collected by a photodiode array and the overall intensity distribution is converted to the size distribution of the droplets along the beam path. The Interferometric Laser Imaging for Droplet Sizing [10-13] technique or ILIDS illuminates a plane of the measured spray by a laser sheet and the scattered light is

imaged by an out of focus camera. The defocused image of each droplet exhibits a fringe pattern and the spacing between the fringes is proportional to the size of each droplet in the image.

The combined Laser Induced Fluorescence and scattered light (LIF/Mie) technique for droplet sizing [14-17] has been proposed for the measurement of the Sauter Mean Diameter (SMD):

$$SMD = \frac{\int_{D=0}^{\infty} D^3 dN(D)}{\int_{D=0}^{\infty} D^2 dN(D)} \quad (1)$$

of spray droplets, where dN(D) is the probability distribution of the spray droplets. The LIF/Mie technique has the significant advantage over other droplet sizing methods in that it is a planar technique that can size full planes of sprays, while the other methods are limited to 'point' (PDA), line of sight (laser diffraction), or planes of small cross sectional areas (ILIDS) of sprays. In addition, this technique is applicable to dense sprays regions, provided appropriate compensation of multiple scattering effects is included.

Essential to the technique is that the liquid is transparent and doped with a fluorescing agent such rhodamine [18-21], fluorescein [22], naphthalene[23] or TMPD [24], which are commonly used in liquid flow diagnostics. A cross section of the spray is illuminated by a laser sheet, usually from an Nd:YAG laser, and one camera records the intensity of the scattered light from the droplets at the laser wavelength and another the intensity of the red shifted fluorescent light from the droplets, as shown in Fig. 1.

The fundamental hypothesis of the LIF/Mie technique for droplet sizing [14, 17] is that when a spherical droplet doped with a fluorescing dye is illuminated with a laser, the intensity of the fluorescent light, $I_f(D)$, from a droplet is proportional to the volume of the illuminated droplet while the intensity of the scattered light, $I_s(D)$, is proportional to the surface area of the illuminated droplet:

$$I_s(D) = a_s D^2 \tag{2}$$

$$I_f(D) = a_f D^3 \tag{3}$$

The ratio of the fluorescent to the scattered light intensities of an ensemble of droplets is then proportional to their SMD:

$$SMD = \frac{\int_{D=0}^{\infty} D^3 dN(D)}{\int_{D=0}^{\infty} D^2 dN(D)} = \frac{\int_{D=0}^{\infty} \frac{1}{a_f} \cdot I_f(D) \cdot dN(D)}{\int_{D=0}^{\infty} \frac{1}{a_s} \cdot I_s(D) \cdot dN(D)} = \frac{1}{K} \cdot \frac{\int_{D=0}^{\infty} I_f(D) \cdot dN(D)}{\int_{D=0}^{\infty} I_s(D) \cdot dN(D)} \tag{4}$$

with K being a constant that is determined from calibration.

The technique has been applied by a number of researchers to characterize sprays [25-32] even in regions when the droplet density makes the application of other laser diagnostic measurements difficult. However, not all researches agree on the correctness of the fundamental hypothesis of the LIF/Mie technique. While the fundamental hypothesis of the LIF/Mie technique is intuitively convincing and in some cases true, it has been demonstrated that its validity is not guaranteed in all situations. For example, the fluorescent light is indeed emitted from within the droplet volume but its intensity distribution has been shown to vary within the droplet volume [33-34]. It has also been demonstrated that the light absorbed by a droplet [29, 35] and the fluorescent light emitted from it [15, 21, 36-37], are not always proportional

to the volume of the droplet. All the effects regarding the absorption and fluorescent light emission from droplets were shown to be significantly influenced by the concentration of the fluorescent dye in the droplet. In addition, while the scattering of light does indeed occur at the droplet surface, it does not occur uniformly across it, as the presence of glare points [38] on the surface of droplets indicates, and the scattered light intensity has also been demonstrated not to be directly proportional to the droplet surface area [21, 36]. Finally, experimental comparison between the LIF/Mie technique and PDA has shown that there is not always agreement between the two [31, 39].

A further issue of the LIF/Mie technique is related to the secondary scattering of light scattered from the illuminated droplets by other droplets present along the path to the camera lens [40-43] which is not negligible and can affect the sizing accuracy. However recent progress has made quantitative measurements possible in dense sprays, where multiple scattering is significant [44-45]. The proposed methods enable us to focus on the investigation of the validity of the fundamental hypothesis on the LIF/Mie technique without considering the effects of multiple scattering, since these can be addressed. Consequently, the LIF/Mie technique can be applicable to a wider range of sprays than before.

The above literature review demonstrates that the fundamental hypothesis of the LIF/Mie technique (i.e. the validity of Eqs. (2) and (3)) is not assured. While it is possible to investigate the accuracy of the LIF/Mie technique by comparing the LIF/Mie and PDA measurements in a spray, this approach has limited scope. A better approach would be to use a controlled group of spheres such as a suspension of polystyrene spheres in water. However due to the sheer number of combinations of

physical parameters that we need to evaluate in order to draw conclusions on the fundamental aspects of the LIF/Mie technique a numerical approach is necessary.

The purpose of this paper is to evaluate the validity of the fundamental hypothesis of the LIF/Mie technique in relation to the various physical parameters that affect it. The paper is structured as follows. In the second section, the numerical approach and the description of the investigated parameters are outlined. In the third section the dependence of the fluorescent and of scattered light intensities is examined systematically as a function of the real refractive index, the dye concentration in the liquid (imaginary part of refractive index) and the light scattering angle and the conditions for which the fundamental hypothesis of the LIF/Mie technique is satisfied are identified. The droplet sizing uncertainty is finally discussed. The paper closes with a summary of the main conclusions.

2. Optical arrangement and investigated parameters

Conceptually the scattering and absorption of light by a spherical droplet can be understood by considering a number of parallel rays that interact with a droplet, as described by the Geometrical Optics, GO, approximation [46]. When these rays reach the surface of the droplet, each ray reflects and refracts on the droplet surface (Fig. 2). The light intensity of the original ray is distributed between the externally reflected ray, designated as light path of order p=0. When the refracted part of the original ray meets the inner droplet surface, a part of its intensity refracts and scatters to the outside and a part of its intensity reflects back inside the droplet and the process is repeated. The refracted ray that is scattered outside the droplet is classified by the number of reflections it has undergone within the droplet as refraction of order p=1,2,3... The intensity of the scattered light collected by a camera placed at an angle θ to the direction of the illumination as defined in Fig. 2, is determined by the sum of the amplitudes of the rays that are scattered from the droplet surface at that angle, considering the phase relations between them, and can include the contributions of multiple orders of refraction.

While the GO approximation is a conceptually useful model and provides an intuitive understanding of the light scattering process by a droplet, it is not perfectly accurate especially when the droplet diameter becomes comparable to the wavelength of the illumination [46]. The exact solution of the scattered and fluorescent light intensities from droplets can be attained by Lorenz-Mie theory [47-49], which is the rigorous solution of Maxwell's equations for the scattering and absorption of a plane wave incident on a spherical droplet. This is the method used in this investigation. The methodology for the implementation of Lorenz-Mie theory that is used here is described in detail by Bohren and Huffman [35].

For reasons of simplicity and because the amount of light emitted as fluorescence is expected to be directly proportional to the amount of light absorbed by the droplet, the absorption cross section:

$$C_{abs} = Q_{abs} \cdot A \tag{5}$$

(with A being the droplet cross section and Q_{abs} being the absorption efficiency of the incident illumination) was used as representative of the fluorescent intensity and will be used synonymously. Certain issues regarding the fluorescence of droplets such as saturation of the fluorescent light intensity due to the intensity of the laser illumination [22] and quenching or temperature effects [19, 23, 50] on the dye fluorescence have been identified previously but will not be considered here as they can be addressed by adjusting the laser intensity and proper selection of a fluorescent dye. The variation of the fluorescent light intensity with the scattering angle around the droplet was not considered. However, it has been demonstrated, for a droplet illuminated by a beam of about a tenth of the droplet diameter, that the variation of the fluorescent light intensity is less than about 10% for the range of scattering angles we investigated [51]. As fully illuminated droplets are considered here, the effect of the scattering angle is negligibly small and does not change our conclusions.

Three parameters have been identified previously [21, 36] as significant to the sizing accuracy of the LIF/Mie technique, but their effect on the LIF/Mie technique has not been systematically investigated. The real refractive index of a liquid, m, the imaginary refractive index of a liquid κ, (whose effects can also be equivalently described by the absorption coefficient of the sprayed liquid γ or the concentration of the fluorescing dye in the sprayed liquid c) and the collection angle θ. The real refractive index of liquids that are used in atomization applications varies widely. For

example it is 1.33 for water, 1.40 for iso-octane and 1.49 for toluene. For this reason, real refractive indices between 1.30 and 1.50 are considered in steps of 0.01 to cover most liquids of interest to atomization applications. Instead of the imaginary refractive index of the liquid, for compatibility with the previous investigations of [21, 36], the concentration of the fluorescing dye (considered fully soluble in the droplet liquid) will be used and Rhodamine 6G with an absorption cross section of $8800m^2$/mole is considered. This approach gives a practical insight on the amount of dye that should be used. Five dye concentrations are examined between c=0.001g/l to c=0.100g/l. For these dye concentrations the absorption coefficient of the sprayed liquid ranges between $18m^{-1}$ to $1837m^{-1}$ and the imaginary refractive index ranges between 7.77e-7 to 7.77e-5.

The angle θ, between the laser sheet and the camera is most often 90º, because the image of the spray is focused across the whole imaged area and no perspective correction is required. However, as the measured spray might be enclosed within a geometry that does not allow optical access with this arrangement, imaging angles in the range between 60º and 120º are considered. Focused imaging of the spray can be obtained by placing the imaging camera and the imaging lens at angles between each other conforming to the Scheimpflug principle [52] and the perspective error can be corrected.

The ranges of values of the above parameters that are considered in this investigation are summarized in Table 1.

Table 1 Ranges of considered parameters

Dye concentration in the droplet liquid c,	0.001 g/l (18.37 m^{-1}, 7.77E-07)
and corresponding absorption coefficient	0.005 g/l (91.87 m^{-1}, 3.88E-06)
and imaginary refractive index	0.010 g/l (183.7 m^{-1}, 7.77E-06)
	0.050 g/l (918.7 m^{-1}, 3.88E-05)
	0.100 g/l (1837 m^{-1}, 7.77E-05)
Real refractive index, m	1.30-1.50 in steps of 0.01
Collection angle, θ	60°-120° in steps of 5°

The Lorenz-Mie theory calculations were performed for droplets of diameter between 1-1000μm to cover the full range of droplets that might be encountered in various types of sprays, considering an illumination wavelength of 532nm, which is commonly used for LIF/Mie measurements.

An additional parameter that influences the scattered light intensity is the solid angle over which the scattered light is collected. Throughout this investigation, the solid angle is fixed at 3.8º. The reason this relatively large solid angle was selected, is that the oscillations of the scattered light intensity that occur with small solid angles (Fig. 3a) are dampened (Fig. 3b) due to averaging across a large solid angle and more accurate results can be obtained.

3. Dependencies of the fluorescent and scattered light intensity from droplets

A. Fluorescent light

The profiles of the fluorescent light intensity of droplets show a high dependence on dye concentration. For each droplet diameter, the absorption cross section and therefore the fluorescent intensity increases with the dye concentration. However, the absolute fluorescent light intensity is not an issue during measurements, unless the signal to noise ratio is low. More important is the relationship with the droplet diameter. For the lowest dye concentration, there is good conformity of the relation of the absorption cross section to the volume of the droplet, which is shown for each condition as a straight line (Fig. 4). For the higher dye concentrations, there is a departure of the desired cubic relationship between the absorption cross section and the droplet diameter, manifested as a change in the slope. This is in agreement with the findings of [21]. As the dye concentration increases the change of slope occurs at increasingly smaller droplets.

Using the method of least squares, the values of the absorption coefficient were fitted to a power law function:

$$I_f = a_f D^{b_f} \tag{6}$$

with a_f and b_f free to take the values that best describe the dependence on droplet diameter. Ideally b_f should be equal to 3. In Fig. 5 the dependence of the value of the exponent b_f is presented for the range of dye concentrations and real refractive indices that were examined. The results indicate an inverse dependence of b_f on dye concentration. For the lowest dye concentration considered, c=0.001g/l, b_f is 2.97.

Although not a perfect match to the expected value of 3, it is very close and signifies a good proportionality between the volume and the fluorescent intensity of a droplet. However, with increasing dye concentration, b_f constantly decreases to 2.95 for c=0.010g/l down to 2.77 for c=0.100g/l where the fluorescent intensity is definitely not proportional to the volume of the droplet. Therefore, it is important that the dye concentration is kept as low as possible so that the relationship between fluorescent intensity and droplet volume is maintained. In contrast to dye concentration, the effects of the real refractive index of the droplets are small and the value of b_f remains almost unchanged within the examined ranges (see Fig. 5).

B. Scattered light

The intensity of the scattered light of droplets, in addition to the refractive index of the droplets and the dye concentration in the liquid, is influenced by the collection angle θ between the direction of the illuminating light and the imaging camera. This is due to the multiple orders of refraction that may or may not contribute to the scattered light at certain angles. The range of angles over which the contribution of each order of refraction becomes insignificant can be described by sharp borders in the GO approximation, which forms a useful basis for the description of the phenomena of this investigation. In reality, there is a gradual reduction of the contribution from each part of the scattered light. Orders up to p=3 are strong and will be used in the description, while orders over p=3 contribute less to the overall scattered light intensity and can be ignored in this description. However, it should be noted that nevertheless all orders, to the accuracy of the numerical implementation of Lorenz-Mie theory, are included in the calculation of the intensity of scattered light. The ranges of influence of each order of refraction are shown in Fig. 6. The only order that contributes at all scattering angles θ is p=0, while p=1 and p=3 contribute mainly in the forward direction and p=2 contributes in the backward direction. Additionally, multiple contributions of p=2 and p=3 are possible at certain scattering angles. The bounds of these ranges and the presence of multiple contributions are determined by the rainbow angles and the edge rays, which in turn depend on the refractive index of the droplets. A thorough explanation of the mechanisms and the associated equations is given in [46].

The orders and the multiplicity of scattered light contributions that make up the overall scattered light intensity depend jointly on the real refractive index m and the

scattering angle θ. Therefore, the m-θ domain was divided into regions on the basis of the orders and multiplicity of scattered light components they include, as shown is Fig. 7. Each grid point in Fig. 7 represents a combination of m and θ, for which calculations of the scattered light intensity were performed. Six regions are present in the range of m and θ:

Region 1. Forward scattering, where the scattered light signal is made up of external reflection, first order refraction and single contribution of the third order refraction.

Region 2. Dominated by external reflection and the second internal reflection

Region 3. The contribution is due to external reflection and dual contribution of the second internal reflection.

Region 4. The scattered light signal is only due to external reflection.

Region 5. Contributions of external reflection, refraction and dual contribution of the second internal reflection.

Region 6. Contributions of external reflection and refraction. However, due to its very limited range of angles and real refractive indices, the phenomena in this region will be described along with those of region 5.

In the same manner as with the fluorescent light intensities, the scattered light intensities were fit to a power law function of the droplet diameter

$$I_s\left(D\right) = a_s D^{b_s} \tag{7}$$

with the a_s and b_s free to take the values that best describe the dependence on the droplet diameter. For the scattered light intensity from the droplets to be proportional to the droplet surface area, b_s should be equal to 2. For the lowest dye concentration, the value of b_s is shown in Fig. 8a as a function of real refractive index of the liquid

and the scattering angle. In most cases, the value of b_s is not 2 and its distribution in the m-θ domain is in accordance with the six regions defined in Fig. 7.

In region 1, b_s is highest at θ=60° for all m and reaches values higher than 1.95 but it does not become equal to 2. The value of b_s decreases in the direction of the refraction edge ray. This implies that b_s is mostly influenced by p=1. At the location of the refraction edge ray, b_s reaches a minimum of about 1.8.

The value of b_s in region 2, where p=1 is suppressed and the scattered light intensity is mainly due to p=0 with a smaller contribution of p=3, is generally above 1.85 and peak values go as high as 1.92.

There is a further increase of b_s in region 3, where the external reflection signal is strengthened by the double contribution of the 2^{nd} internal reflection. Close to the second rainbow angle, b_s is especially high, marginally exceeding 2 in some cases. However, any deviation of the value of b_s from 2 means that the scattered light intensity is not proportional to the surface area and, as a consequence, the sizing uncertainty of the LIF/Mie technique should increase in this case as well. There are, however, combinations of m and θ, where b_s is exactly 2. Sizing of droplets with the LIF/Mie technique for these particular combinations will result in negligible sizing error. However, the extent of the locus of these regions is somewhat narrow and in practice it might be difficult to attain the precise combination of m-θ that result in b_s being exactly 2.

In region 4, the dual contribution of the second internal reflection is suppressed and b_s decreases sharply close to the second rainbow angle from over 2 to 1.8. Farther from the second rainbow angle the value of b_s recovers and with the p=0 part being the only significant contribution to the scattered light, b_s exceeds 1.9. The value of b_s shows that the relationship between the scattered light intensity and the droplet surface area

is not perfect. However, there is little variation of b_s for most of region 4, which could make this region attractive for LIF/Mie sizing measurements.

The distribution of b_s in regions 5 and 6 is an amalgamate of regions 1 and 3 and is influenced by all scattered light contributions that are present in regions 1-4. The value of b_s decreases as the scattering angle approaches the refraction edge ray. There is an increase of the values of b_s close to the second rainbow angle. For most of this region b_s is below 1.9.

A consideration regarding the modeling of $I_s(D)$ according to the power law of Eq (7) is that the scattered light intensity shows oscillations around the main trend with amplitude that can vary considerably with the refractive index of the droplet and the scattering angle. This is demonstrated by comparison of the scattered light intensity, $I_s(D)$, from droplets of m=1.41, imaged at θ=60° (Fig. 9a) and θ=90° (Fig. 9b). At θ=60°, there is a smooth increase of the scattered light intensity with the droplet diameter while at θ=90° the increase of the scattered light intensity with the droplet diameter is highly irregular. The observed oscillations of the scattered light intensity were verified to be independent of the number of nodes of the numerical integration of the scattered light intensity across the imaging aperture. They represent therefore a real effect, which will influence the sizing accuracy of the LIF/Mie technique.

The coefficient of determination:

$$R^2 = 1 - \frac{SS_{err}}{SS_{tot}} \tag{8}$$

with SS_{err} being the sum of squared residuals and SS_{tot} being the total sum of squares of the power law fit of $I_s(D)$ as a function of the droplet diameter, is representative of the quality of the fit of $I_s(D)$ to the power law and is presented in Fig. 8b. The values of R^2 are very high throughout, indicating that the power law functions are a good

description of the relation between $I_s(D)$ and droplet diameter. However, the lower values of R^2 in the m-θ domain can identify the combinations of droplet refractive index and scattering angle where the amplitude of the oscillations of the scattered light intensity is high.

The oscillations of the scattered light intensity, $I_s(D)$, appear to be larger (lower R^2) at two locations of the m-θ domain. One at scattering angles around $90°$, extending over a large range of refractive indices. This is a significant problem for the application of the LIF/Mie technique, as imaging normal to the laser sheet is the most convenient way. The second locus of decreased values of R^2 is for droplets of refractive indices around 1.4 and extends to most imaging angles. This is also of concern because the liquid fuels with significant interest to atomization studies such as kerosene, iso-octane, decane and dodecane are affected. The only way to avoid this problem is by obtaining the scattered light images of sprays of these liquids at forward (i.e $\theta<65°$) or backward (i.e $\theta>118°$) scattering angles that remain unaffected. Imaging at these angles is possible if the camera lens is mounted on the camera in accordance to the Scheimpflug principle to enable focused imaging.

Increasing the dye concentration in the liquid to c=0.010g/l (an order of magnitude greater to that of Fig. 8a), there are some changes in the distribution of the values of b_s in the m-θ domain, as shown in Fig. 10a. The value of b_s is generally lower than 2 throughout the domain due to the increased absorption of the incident illumination within the droplet. Regions 1, 5 and 6 are significantly affected as p=1 (refraction) is a major contributor. Nevertheless, despite the decrease, the value of b_s is consistently over 1.90 at $\theta=60°$ for all values of the refractive index. Region 2 is not affected greatly, since p=1 is suppressed there, while p=0 is dominant and b_s is generally above 1.85. In Region 3, where there is a dual contribution of p=2, there is a decrease

in the value of b_s in comparison to the lower dye concentration close to the second rainbow angle, where b_s drops from above 2 to about 1.97, and throughout the rest of the region b_s drops to about 1.85. In region 4, with p=1 being the only contribution to the scattered light intensity (disregarding contributions with values of p greater than 3) there is small decrease in b_s.

The value of R^2 is also affected, as shown in Fig. 10b. Qualitatively, its distribution in the domain of the real refractive index and the scattering angle does not change compared to the lower dye concentration (Fig. 8) and the problematic regions remain around θ=90° and around m=1.4. However, quantitatively there is a small overall increase in the value of R^2. Due to the increase of light absorption within the droplets, there is increased suppression of the intensity of the higher orders of refraction. Consequently, the interference effects between the various orders of refraction become less important and the magnitude of the oscillations of the scattered light intensity around the mean trend is reduced. However, the decrease of the magnitude of the oscillations is relatively small, which can be confirmed by comparison of the magnitude of the oscillations of the scattered light intensity for c=0.010g/l of Fig. 11 and for c=0.001g/l of Fig. 9a.

For the highest dye concentration of c=0.100g/l, there is a significant reduction to the value of b_s to below 1.8 for regions 1, 3, 5 and 6 (see Fig. 12a), where refraction is more heavily affected. The values of b_s in these regions are unacceptable for sizing measurements, since the relation between $I_s(D)$ and droplet surface area is invalidated. In contrast in region 4, where $I_s(D)$ is almost exclusively due to p=0, b_s remains above 1.9. Similarly in region 2, where $I_s(D)$ is mainly due to p=0 and to a lesser extent p=3, b_s remains above 1.85.

Despite the reduction of the exponent b_s due to the increase of the dye concentration in the droplets, the quality of the fitting of $I_s(D)$ to power law functions of the droplet diameter improves in most cases and the value of R^2 (Fig. 12b) is generally greater for most combinations of the refractive index and the scattering angle for c=0.100g/l than for c=0.010g/l (Fig. 10b). This is due to the heavy suppression of the oscillations of the scattered light intensity around the main trend, which is demonstrated by the profile of $I_s(D)$ in Fig. 13. The increase of the values of R^2 is especially profound around m=1.41 and θ=90°, where the oscillations of $I_s(D)$ were also large at the lower dye concentrations. Some decrease of R^2 nevertheless can be observed along the second rainbow angle (dashed line of Fig. 12b) and around θ=60° for m>1.40, where $I_s(D)$ is significantly affected due to the increased absorption within the droplets.

C. Overview of the effect of the experimental conditions on the conformity of the fluorescent and scattered light intensities to the fundamental hypothesis of the LIF/Mie technique.

It was stated at the beginning of the paper that the fundamental hypothesis of the LIF/Mie technique requires that the fluorescent and scattered light intensities from the droplets are proportional to the volume and surface area of the droplets respectively. The fitting of the fluorescent light intensity of droplets in the 1-1000μm diameter range to power law functions of their diameter (Eq. (6)) showed that the power law exponent, b_f, is highly dependent on dye concentration in the liquid and minimally dependent on the refractive index of the liquid. Its value can range from about 2.97, which demonstrates a close correspondence between the fluorescent light intensity

and droplet volume down to about 2.77 where the aforementioned relationship becomes questionable.

The fitting of the scattered light intensity of the droplets to a power law function of their diameter (Eq. (7)) showed that the value of the power law exponent, b_s, is highly susceptible to the dye concentration in the liquid, the real refractive index of the liquid and the scattering angle. Exponent b_s, was found to range from slightly over 2 to below 1.7. Therefore, the scattered light intensity is a good indication of the surface area of the droplets only for a limited range of dye concentrations, real refractive indices and scattering angles, where b_s is close to 2. In addition to the conformity of the scattered light intensity to the surface area of the droplets, as described by the power law, a further complication in the LIF/Mie technique arises from the oscillations of the scattered light intensity of the droplets around the power law. These oscillations, which are due to interference between the different orders of refraction that contribute to the scattered light intensity, cause droplets of similar diameters (hence surface areas) to have markedly different scattered light intensities. These are due to a resonator effect, which scales with droplet diameter, caused by the interference of different orders of refraction. As a result, the relationship between the scattered light intensity and droplet surface area becomes non-monotonic.

As a consequence of the above, the direct proportionality between the LIF/Mie intensity ratio and droplet diameter, expected from Eq. (4), is only valid in cases where both the fluorescent and the scattered light exponents obtain values close to 3 and 2 respectively and the scattered light intensity does not exhibit significant oscillations with droplet size. An example of such a case is demonstrated in Fig. 14a. The power law best fit of the $I_s(D)/I_f(D)$ ratio to droplet diameter results to a power law exponent of 0.995, which confirms an almost perfect linear relationship between

the LIF/Mie ratio and droplet diameter. The correspondence is good even for small droplets in the range of 0-100 micron as can be seen in the insert. In such a case, the LIF/Mie technique produces reliable results with low sizing uncertainty.

In contrast, the LIF/Mie intensity ratio is not a good indication of droplet diameter in cases where either the fluorescent or the scattered light exponents do not obtain values close to 3 and 2 respectively or if the scattered light intensity exhibits oscillations with droplet diameter. This is demonstrated in the example of Fig. 14b, where the best power law fit of the LIF/Mie intensity ratio to droplet diameter results to an exponent of 1.159, which indicates a non-linear relationship between the LIF/Mie intensity ratio and droplet diameter. In addition, the LIF/Mie intensity ratio exhibits large oscillations of its magnitude due to the oscillations of the scattered light intensity and as a result there is not a monotonic relation between LIF/Mie intensity ratio and droplet diameter. In the example of Fig. 14, droplets with diameters between 600μm and 800μm can have the same LIF/Mie intensity ratio. Therefore, in this case LIF/Mie measurements will not produce accurate droplet sizing results.

Since the LIF/Mie intensity ratio of the measured droplets depends on the dye concentration in the liquid, the droplet refractive index and the scattering angle, it is necessary to identify the particular combinations of these parameters for which the fundamental hypothesis of the LIF/Mie technique is valid and accurate droplet sizing measurements can be obtained.

The refractive index of the droplets has little effect on fluorescent light intensities. However, the refractive index and the scattering angle determine which orders of refraction contribute to the scattered light intensity. As such, they are the defining parameters regarding both the conformity of the scattered light intensities to the surface area of droplets and the existence of oscillations of scattered light intensity

and need to be considered concurrently. From the perspective of the conformity of scattered light intensity to droplet surface area, the best possible combination of refractive index and scattering angle is along the second rainbow angle where the exponent b_s becomes exactly 2. Along this region of the m-θ domain the LIF/Mie technique is expected to produce very accurate measurements. However, small uncertainties of either m or θ along the second rainbow angle result in large changes of the exponent b_s, which makes the practical implementation of the LIF/Mie technique at this region problematic. A more attractive region for LIF/Mie measurements is at the forward scattering region for all droplet refractive indices where the scattered light intensity conforms well to the fundamental hypothesis of the LIF/Mie technique throughout the range of refractive indices considered. In dense sprays, due to multiple scattering, the contribution of higher orders of refraction to the overall scattered light intensity could increase, causing the scattered light exponents to change. While it could be hypothesized that there will be cases where the exponents would obtain values closer to the ideal, this is not guaranteed. In addition, as the droplet number density can vary from shot to shot during measurements, the contribution of higher orders of refraction would not be constant. This would result to a varying exponent during the measurement, increasing sizing uncertainty. Since multiple scattering is known to cause additional sizing errors, as explained in the introduction, the best sizing strategy is to use, when necessary, methods that compensate for its contribution and rely on singly scattered light from the spray droplets. Considering the oscillations of the scattered light intensity, two regions in the m-θ domain were identified as less favorable due to large amplitude of the oscillations of the scattered light intensity that contradict a monotonic relationship between scattered light intensity and droplet diameter. One related to refractive

indices around 1.4 and one related to scattering angles in the sidescatter direction (around 90°). Both of these regions are best avoided for sizing measurements at present. However as femto-second lasers become more widely available it could be possible to use laser pulses shorter than the droplet diameter to prevent interference between the different orders of refraction and dampen these oscillations [53] This approach requires further research before it becomes applicable.

When considering the dye concentration in the liquid, from the perspective of the fluorescent intensity of the droplets the closest proportionality to droplet volume is achieved for the lowest examined dye concentration. The same is true for the relationship between the scattered light intensities to droplet surface area. Therefore, the lowest dye concentration is warranted for the closest conformity to the fundamental hypothesis of the LIF/MIE technique. This study is focused on Rhodamine 6G illuminated at 532nm, but other dyes are also likely to be used. For reference, the corresponding absorption coefficient for this dye concentration is presented in Table 2 for the dye concentration of 0.001g/l. As the absorption coefficient is close to that of Rhodamine 6G, the conformity to the fundamental hypothesis will be good at this dye concentration for the other dyes as well. The change of the illumination wavelength that is required to excite the different dyes will have an effect on the absolute scattered light intensity but as both the scattered light intensity and the size parameter are change simultaneously, the scaling to the droplet diameter will not be qualitatively affected and the optimal combinations of refractive index and scattering angle identified above will remain the same.

Table 2 Absorption coefficient for various dyes

Dye	Concentration (g/l)	Wavelength (nm)	Absorption coefficient (m^{-1})

Disodium fluorescein	0.001	514	9.2
Naphthalene	0.001	266	4.2
Rhodamine B	0.001	532	17.1

The amplitude of the oscillations of the scattered light intensity was demonstrated to reduce as the dye concentration increases. Nevertheless significant dampening of the oscillations in the sidescatter direction and for liquids with refractive indices of 1.4, for which the amplitude was found to be considerable, occurred for dye concentrations of 0.1g/l as evidenced by the increase of the magnitude of the coefficient of determination R^2 at this dye concentration. In such cases, however, the fundamental hypothesis of the LIF/Mie technique is invalidated for both the fluorescent and the scattered light. Consequently, it is recommended that the dye concentration in the liquid remain minimal and the LIF/Mie technique is applied for combinations of m and θ where the amplitude of the scattered light oscillations is minimal.

4. Conclusions

The dependency of the fluorescent and scattered light intensities from illuminated droplets on droplet diameter was examined using Mie theory calculations as a function of the real refractive index of the droplets in the range of 1.30 to 1.50, the concentration of the fluorescent dye in the liquid in the range between 0.001g/l to 0.100g/l (18.37 m^{-1} to 1837 m^{-1}) and the scattering angle in the range between 60° and 120°. This was used to assess the validity of the fundamental hypothesis of the Laser Induced fluorescence and Scattered light (LIF/Mie) technique for planar droplet sizing, which is that the scattered and fluorescent light intensities of spray droplets that are doped with a fluorescing dye and are illuminated by laser light are directly proportional to the surface area and the volume of the droplets respectively. It was found that:

1. The relationship between fluorescent light intensities and droplet volume is closest matched for the lowest fluorescent dye concentration in the liquid (c=0.001g/l of Rhodamine 6G or γ=18.37 m^{-1}).
2. The real refractive index of the liquid has little effect on the relationship between fluorescent light intensity and droplet diameter.
3. The relationship between scattered light intensity and droplet surface area is complex and depends strongly on the real refractive index, scattering angle and dye concentration in the liquid. The best conformity of scattered light intensity and droplet surface area is obtained for the lowest dye concentrations. Exact matching of the scattered light intensity to the surface area of droplets was found along the second rainbow angle. However, the relationship changes rapidly with small changes of either m or θ and the application of the LIF/Mie technique in this

region could be problematic. Very good conformity between scattered light intensities and the surface area of droplets was also observed for all the droplet refractive indices examined in the forward scattering direction at $\theta=60°$, where the sizing uncertainty is expected to be small.

4. The scattered light intensity was found to be affected by intensity oscillations around the best fit power law function. The oscillations are more profound at imaging angles close to the sidescatter location and for liquids with real refractive indices around 1.4. These oscillations can cause problems to the interpretation of the scattered light intensities as they invalidate the relationship between scattered light intensity and droplet surface area. The LIF/Mie technique is best applied outside these combinations of real refractive index and imaging angle.

References

1. F. Durst and M. Zare, "Laser Doppler measurements in two-phase flows," in *The accuracy of Flow measurements by Laser Doppler methods: Proceedings of the LDA Symposium,* (Copenhagen, 1975), pp. 403-429.
2. K. Bauckhage and H. Flogel, "Simultaneus measurement of droplet size and velocity in nozzle sprays," in *Second International Symposium of Laser Techniques to fluids mechanics,* (1984).
3. W. D. Bachalo and M. J. Houser, "Phase Doppler Spray Analyzer for Simultaneous Measurements of Drop Size and Velocity Distributions," Optical Engineering **23**, 583-590 (1984).
4. Y. Hardalupas and A. M. K. P. Taylor, "Phase Validation Criteria of Size Measurements for the Phase Doppler Technique," Experiments in Fluids **17**, 253-258 (1994).
5. Y. Hardalupas and A. M. K. P. Taylor, "The Identification of LDA Seeding Particles by the Phase-Doppler Technique," Experiments in Fluids **6**, 137-140 (1988).
6. R. A. Dobbins, L. Crocco, and I. Glassman, "Measurement of mean particle sizes of sprays from diffractively scattered light," AIAA Journal **1**, 1882-1886 (1963).
7. A. A. Hamidi and J. Swithenbank, "Treatment of Multiple-Scattering of Light in Laser Diffraction Measurement Techniques in Dense Sprays and Particle Fields," J I Energy **59**, 101-105 (1986).
8. L. G. Dodge, "Calibration of the Malvern Particle Sizer," Applied Optics **23**, 2415-2419 (1984).
9. E. Cossali and Y. Hardalupas, "Comparison between Laser Diffraction and Phase Doppler-Velocimeter Techniques in High Turbidity, Small Diameter Sprays," Experiments in Fluids **13**, 414-422 (1992).
10. M. Maeda, Y. Akasaka, and T. Kawaguchi, "Improvements of the interferometric technique for simultaneous measurement of droplet size and velocity vector field and its application to a transient spray," Experiments in Fluids **33**, 125-134 (2002).
11. A. R. Glover, S. M. Skippon, and R. D. Boyle, "Interferometric laser imaging for droplet sizing: A method for droplet-size measurement in sparse spray systems," Appl Optics **34**, 8409-8421 (1995).
12. M. Maeda, T. Kawaguchi, and K. Hishida, "Novel interferometric measurement of size and velocity distributions of spherical particles in fluid flows," Measurement Science & Technology **11**, L13-L18 (2000).
13. Y. Hardalupas, S. Sahu, A. M. K. P. Taylor, and K. Zarogoulidis, "Simultaneous planar measurement of droplet velocity and size with gas phase velocities in a spray by combined ILIDS and PIV techniques," Experiments in Fluids **49**, 417-434 (2010).
14. T. Kamimoto, "Diagnostics of Transient Sprays by Means of Laser Sheet Techniques," in *COMODIA 94,* (1994), pp. 33-41.
15. P. Le Gal, "Laser Sheet Dropsizing of dense sprays," Optics and laser technology **31**, 75-83 (1999).
16. S. V. Sankar, K. E. Maher, and D. M. Robart, "Rapid characterization of fuel atomizers using an optical patternator," Journal of Engineering for Gas Turbines and Power-Transactions of the ASME **121**, 409-414 (1999).

17. C. N. Yeh, H. Kosaka, and T. Kamimoto, "A fluorescence / scattering imaging technique for instantaneous 2-D measurements of particle size distribution in a transient spray," in *Proceedings of the 3rd Congress on Optical Particle Sizing*, (1993), pp. 355-361.
18. P. Lavieille, F. Lemoine, G. Lavergne, and M. Lebouche, "Evaporating and combusting droplet temperature measurements using two-color laser-induced fluorescence," Experiments in Fluids **31**, 45-55 (2001).
19. I. Duwel, J. Schorr, J. Wolfrum, and C. Schulz, "Laser-induced fluorescence of tracers dissolved in evaporating droplets," Applied Physics B-Lasers and Optics **78**, 127-131 (2004).
20. L. A. Melton and C. W. Lipp, "Criteria for quantitative PLIF experiments using high-power lasers," Experiments in Fluids **35**, 310-316 (2003).
21. R. Domann and Y. Hardalupas, "A study of parameters that influence the accuracy of the Planar Droplet Sizing (PDS) technique," Particle & Particle Systems Characterization **18**, 3-11 (2001).
22. K. Jung, H. Koh, and Y. Yoon, "Assessment of planar liquid-laser-induced fluorescence measurements for spray mass distributions of like-doublet injectors," Measurement Science & Technology **14**, 1387-1395 (2003).
23. M. Winter and L. A. Melton, "Measurement of Internal Circulation in Droplets Using Laser-Induced Fluorescence," Appl Optics **29**, 4574-4577 (1990).
24. K. Matsumoto, T. Fujii, M. Suzuki, D. Segawa, and T. Kadota, "Laser-induced fluorescence for the non-intrusive diagnostics of a fuel droplet burning under microgravity in a drop shaft," Measurement Science & Technology **10**, 853-858 (1999).
25. B. D. Stojkovic and V. Sick, "Evolution and impingement of an automotive fuel spray investigated with simultaneous Mie/LIF techniques," Applied Physics B-Lasers and Optics **73**, 75-83 (2001).
26. M. C. Jermy and D. A. Greenhalgh, "Planar dropsizing by elastic and fluorescence scattering in sprays too dense for phase Doppler measurement," Applied physics.B, Lasers and optics **71**, 703-710 (2000).
27. S. Park, H. Cho, I. Yoon, and K. Min, "Measurement of droplet size distribution of gasoline direct injection spray by droplet generator and planar image technique," Measurement Science & Technology **13**, 859-864 (2002).
28. L. Zimmer, R. Domann, Y. Hardalupas, and Y. Ikeda, "Simultaneous laser-induced fluorescence and Mie scattering for droplet cluster measurements," Aiaa Journal **41**, 2170-2178 (2003).
29. M. M. Zaller, R. C. Anderson, Y. R. Hicks, and R. J. Locke, "Comparison of techniques for non-intrusive fuel drop size measurements in a subscale gas turbine conbustor," (1999).
30. S. H. Jin, "An experimental study of the spray from an air-assisted direct fuel injector," Proceedings of the Institution of Mechanical Engineers; Part D; Journal of automobile engineering **222**, 1883-1894 (2008).
31. L. Zimmer and Y. Ikeda, "Planar droplet sizing for the characterization of droplet clusters in an industrial gun-type burner," Particle & Particle Systems Characterization **20**, 199-208 (2003).
32. R. Domann and Y. Hardalupas, "Characterisation of spray unsteadiness," in *ILASS-Europe*, 2002), 287-292.
33. R. Domann and Y. Hardalupas, "Spatial distribution of fluorescence intensity within large droplets and its dependence on dye concentration," Appl Optics **40**, 3586-3597 (2001).

34. R. Domann, Y. Hardalupas, and A. R. Jones, "A study of the influence of absorption on the spatial distribution of fluorescence intensity within large droplets using Mie theory, geometrical optics and imaging experiments," Measurement Science & Technology **13**, 280-291 (2002).
35. C. F. Bohren and D. R. Huffman, *Absorption and scattering of light by small particles* (Wiley-Interscience, New York, 1983).
36. G. Charalampous, Y. Hardalupas, and A. M. K. P. Taylor, "Optimisation of the droplet sizing accuracy of the combined scattering (mie)/Laser Induced Fluorescence (LIF) technique," in *Twelfth International Symposium of Laser Techniques to fluids mechanics*, 2004),
37. B. Frackowiak and C. Tropea, "Numerical analysis of diameter influence on droplet fluorescence," Appl Optics **49**, 2363-2370 (2010).
38. H. C. van de Hulst and R. T. Wang, "Glare Points," Appl Optics **30**, 4755-4763 (1991).
39. R. Domann and Y. Hardalupas, "Quantitative measurement of planar droplet Sauter Mean Diameter in sprays using Planar Droplet Sizing," Particle & Particle Systems Characterization **20**, 209-218 (2003).
40. E. Berrocal, I. Meglinski, and M. Jermy, "New model for light propagation in highly inhomogeneous polydisperse turbid media with applications in spray diagnostics," Optics Express **13**, 9181-9195 (2005).
41. V. Sick and B. Stojkovic, "Attenuation effects on imaging diagnostics of hollow-cone sprays," Applied Optics **40**, 2435-2442 (2001).
42. D. Stepowski, O. Werquin, C. Roze, and T. Girasole, "Account for extinction and multiple scattering in planar droplet sizing of dense sprays," in *Thirteenth International Symposium of Laser Techniques to fluids mechanics*, (2006).
43. L. Araneo and R. Payri, "Experimental quantification of the planar droplet sizing. Technique error for micro-metric mono-dispersed spherical particles.," in *ILASS 2008*, (Como Lake, Italy, 2008).
44. E. Berrocal, E. Kristensson, M. Richter, M. Linne, and M. Alden, "Application of structured illumination for multiple scattering suppression in planar laser imaging of dense sprays," Optics Express **16**, 17870-17881 (2008).
45. E. Kristensson, E. Berrocal, R. Wellander, M. Ritcher, M. Aldén, and M. Linne, "Structured illumination for 3D Mie imaging and 2D attenuation measurements in optically dense sprays," Proceedings of the Combustion Institute **33**(2011).
46. H. C. van de Hulst, *Light Scattering by small particles* (Dover publications, 1957).
47. L. Lorenz, "Lysbevaegelsen i og uden for en af plane Lysbolger belyst Kulge," Det Kongelige Danske Videnskabernes Selskabs Skrifter **6**, 1-62 (1890).
48. L. Lorenz, "Sur la lumiere reflechie et refractee par une sphere transparente," in *Oeuvres scientifiques de L. Lorenz, revues et annotees par H. Valentiner* (Librairie Lehmann et Stage, 1898).
49. G. Mie, "Beitrage zur Optik truber Medien, speziell kolloidaler Metallosungen," Annalen der Physic **25**, 377-455 (1908).
50. I. Duwel, J. Schorr, P. Peuser, P. Zeller, J. Wolfrum, and C. Schulz, "Spray diagnostics using an all-solid-state Nd : YAlO3 laser and fluorescence tracers in commercial gasoline and diesel fuels," Applied Physics B-Lasers and Optics **79**, 249-254 (2004).
51. B. Frackowiak and C. Tropea, "Fluorescence modeling of droplets intersecting a focused laser beam," Opt Lett **35**, 1386-1388 (2010).

52. T. Scheimpflug, "Improved Method and Apparatus for the Systematic Alteration or Distortion of Plane Pictures and Images by Means of Lenses and Mirrors for Photography and for other purposes," GB Patent No. 1196 (1904).
53. S. Bakic, C. Heinisch, N. Damaschke, T. Tschudi, and C. Tropeal, "Time integrated detection of femtosecond laser pulses scattered by small droplets," Appl Optics **47**, 523-530 (2008).

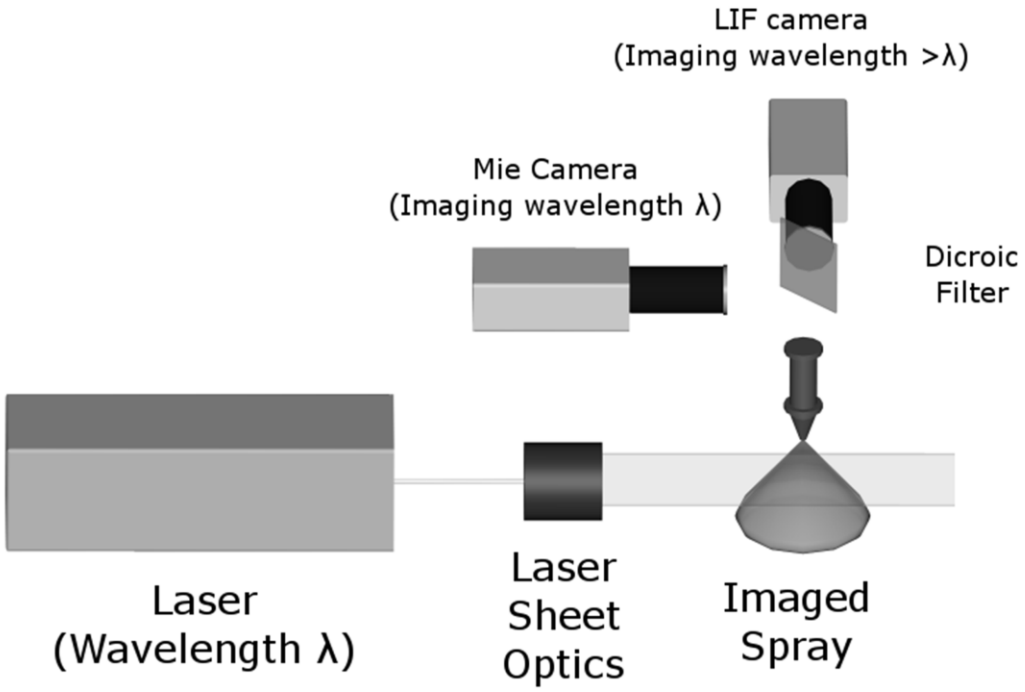

Fig. 1 Example of the experimental arrangement of the LIF/Mie technique

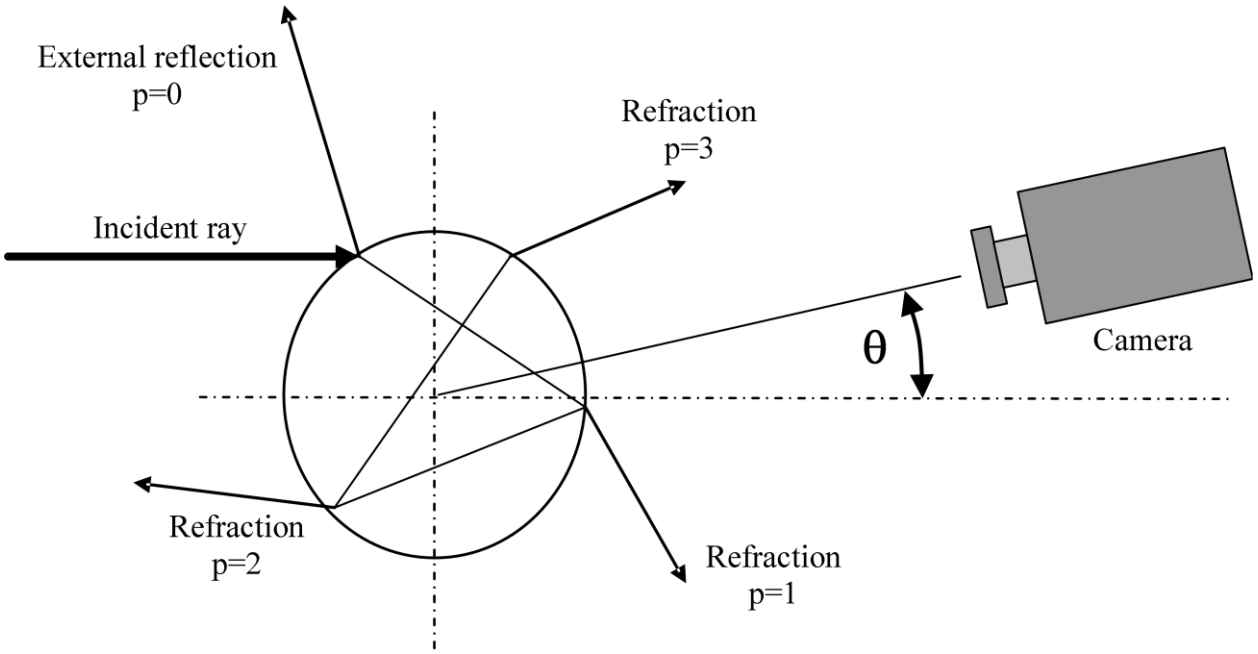

Fig. 2 Scattering of a light ray at the interface of a droplet.

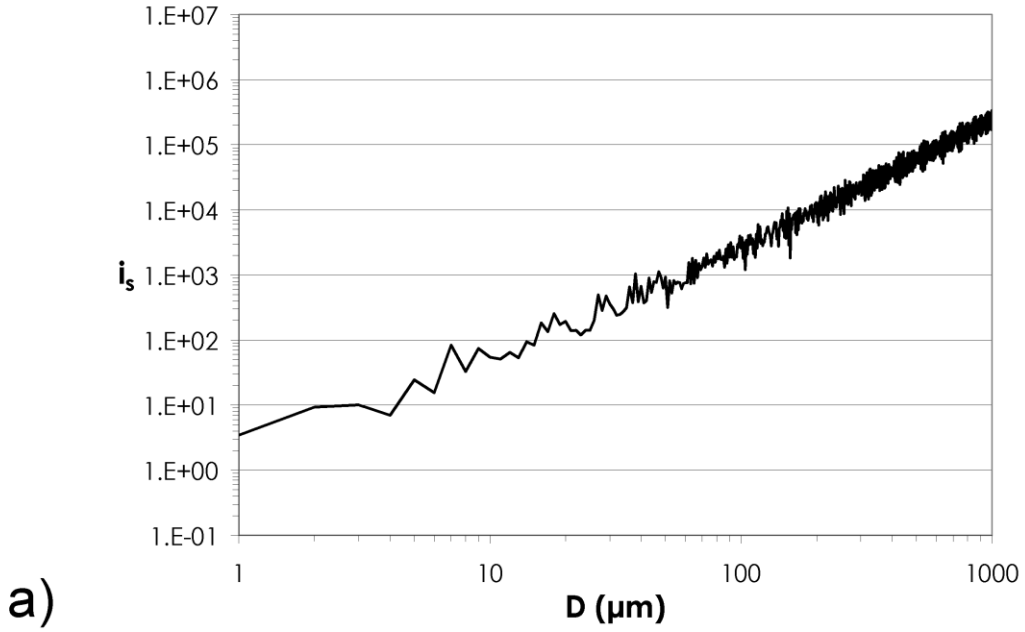

a)

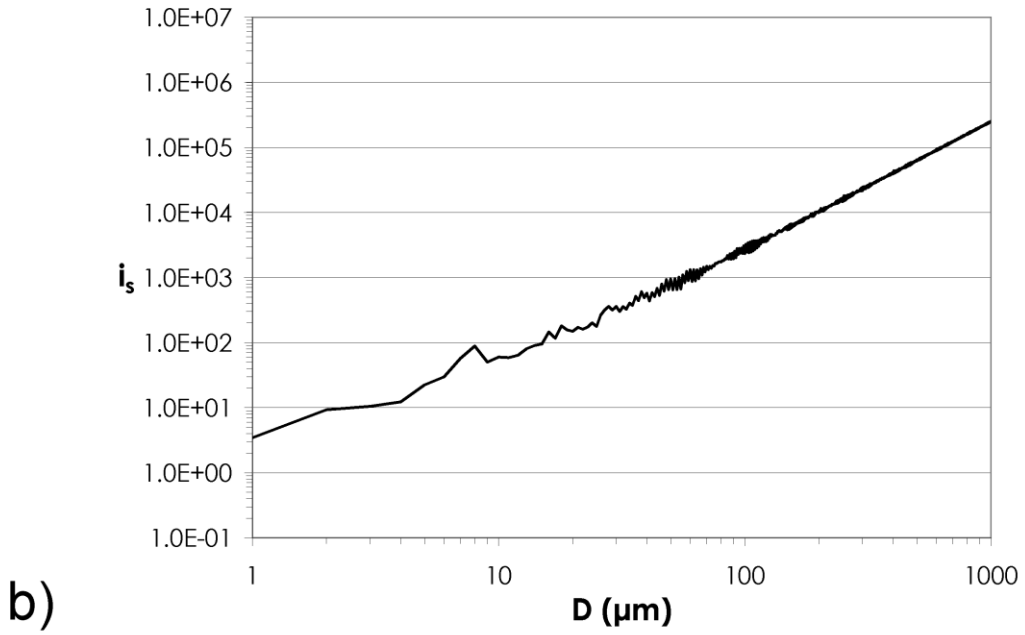

b)

Fig. 3 Scattered light intensity collected by a) an infinitely small solid angle b) a solid angle of 3.8°. The significant oscillations of the scattered light intensity around the main trend that exist when light is collected by an infinitely small aperture are dampened when the light is collected. Calculations for m=1.33, c=0.001g/l and θ=90°.

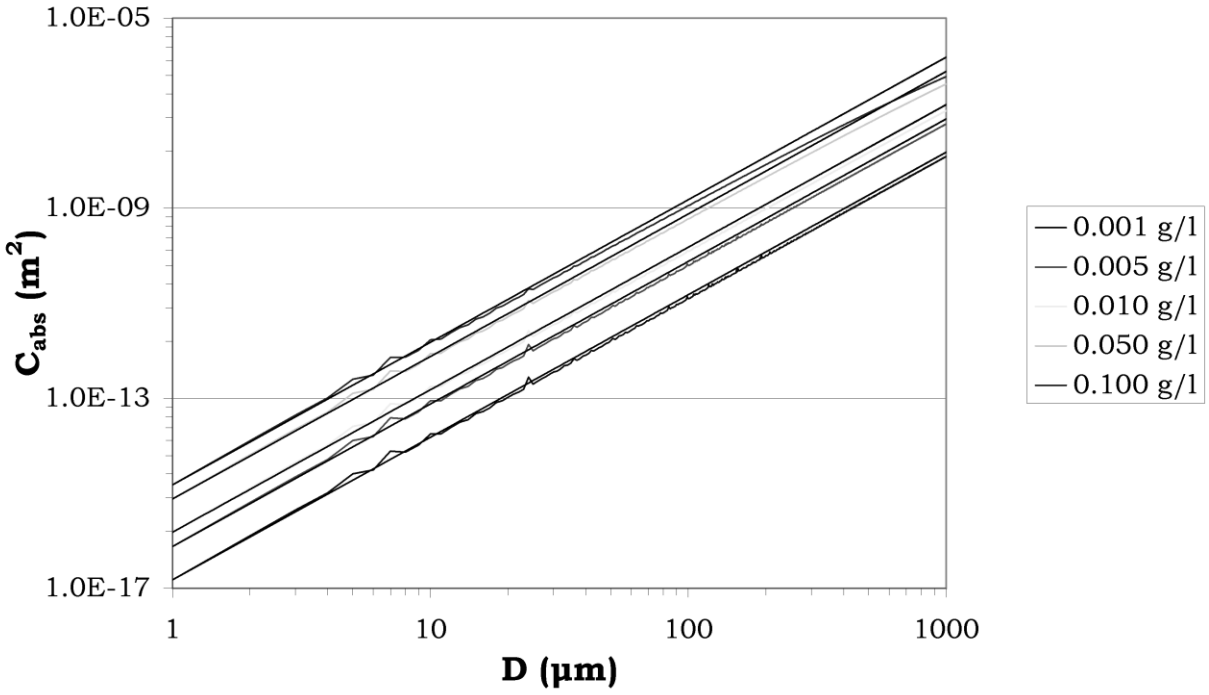

Fig. 4 Absorption cross section of droplets as a function of droplet diameter from low, c=0.001g/l, to high, c=0.100g/l, dye concentrations for m=1.30.

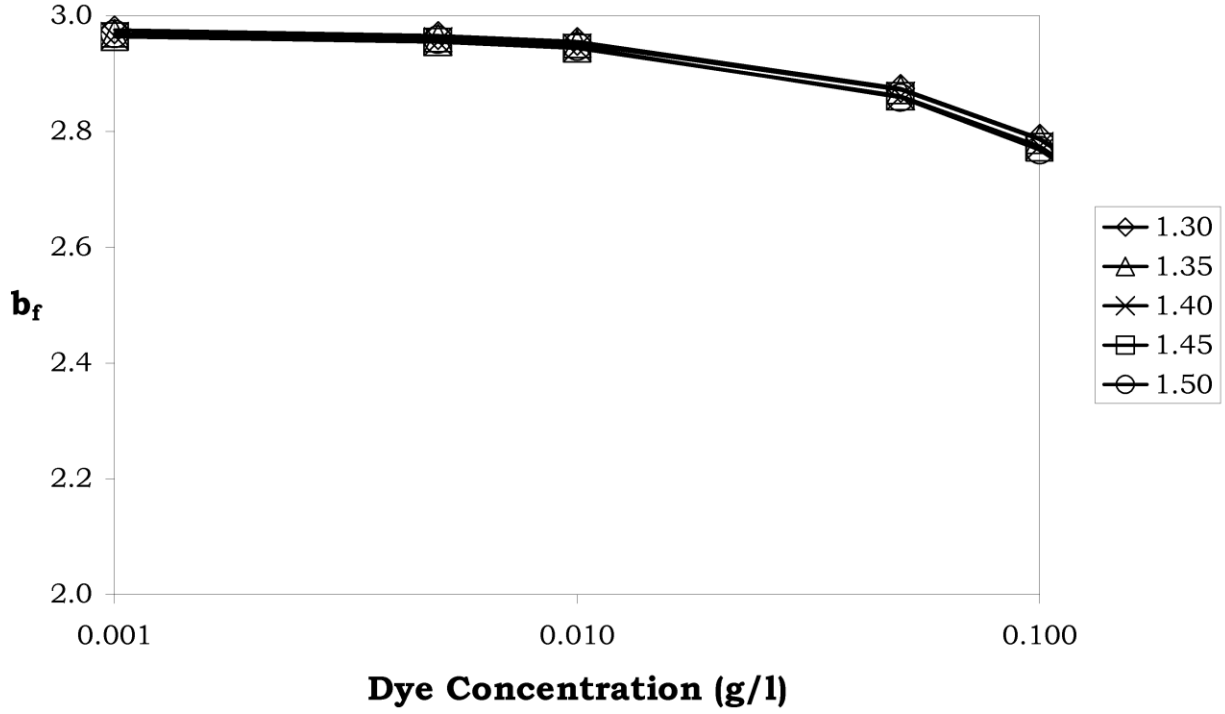

Fig. 5 Exponent b_f of Eq. (3) as a function of dye concentration in the liquid for different values of the real refractive index. Lowest dye concentrations result to closest matching of b_f to the ideal value of 3.

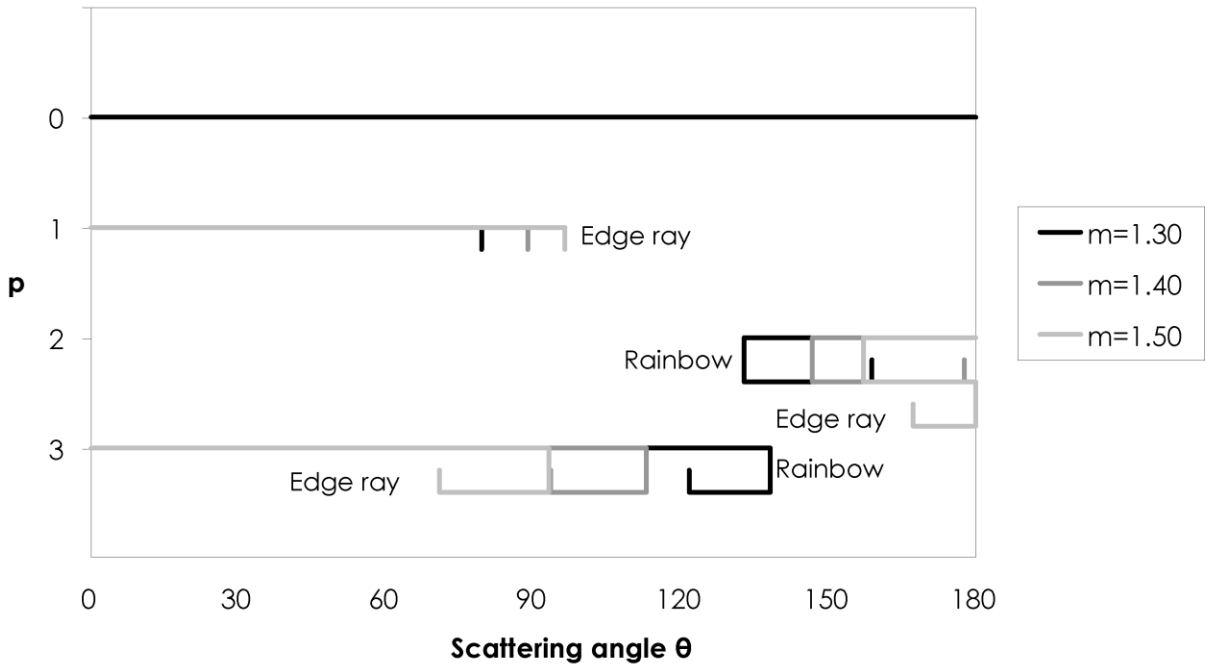

Fig. 6 Region of influence of scattered light components (diffraction and external reflection p=0, refraction p=1, 1st internal reflection p=2, 2nd internal reflection p=3). Folding of lines indicates multiple contribution of the scattered light component.

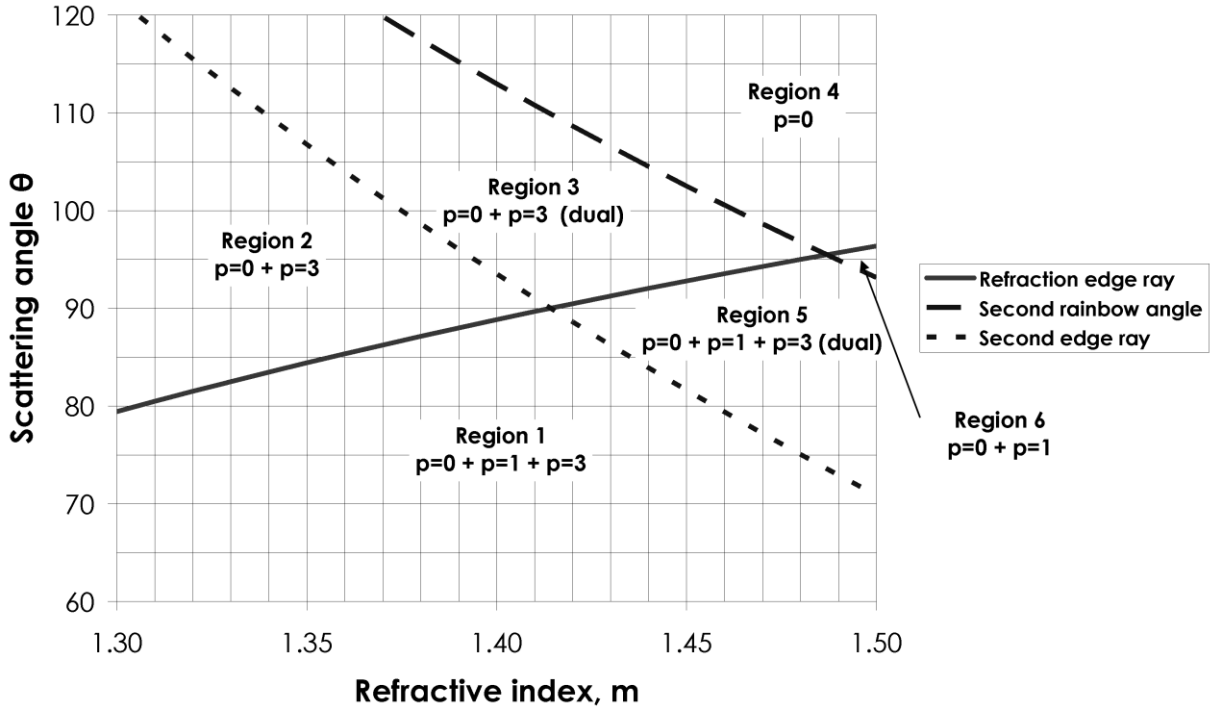

Fig. 7 Real refractive index and scattering angle (m-θ) domain divided into 6 regions depending on the contributions of the components of scattered light (diffraction and external reflection p=0, refraction p=1, 1st internal reflection p=2, 2nd internal reflection p=3)

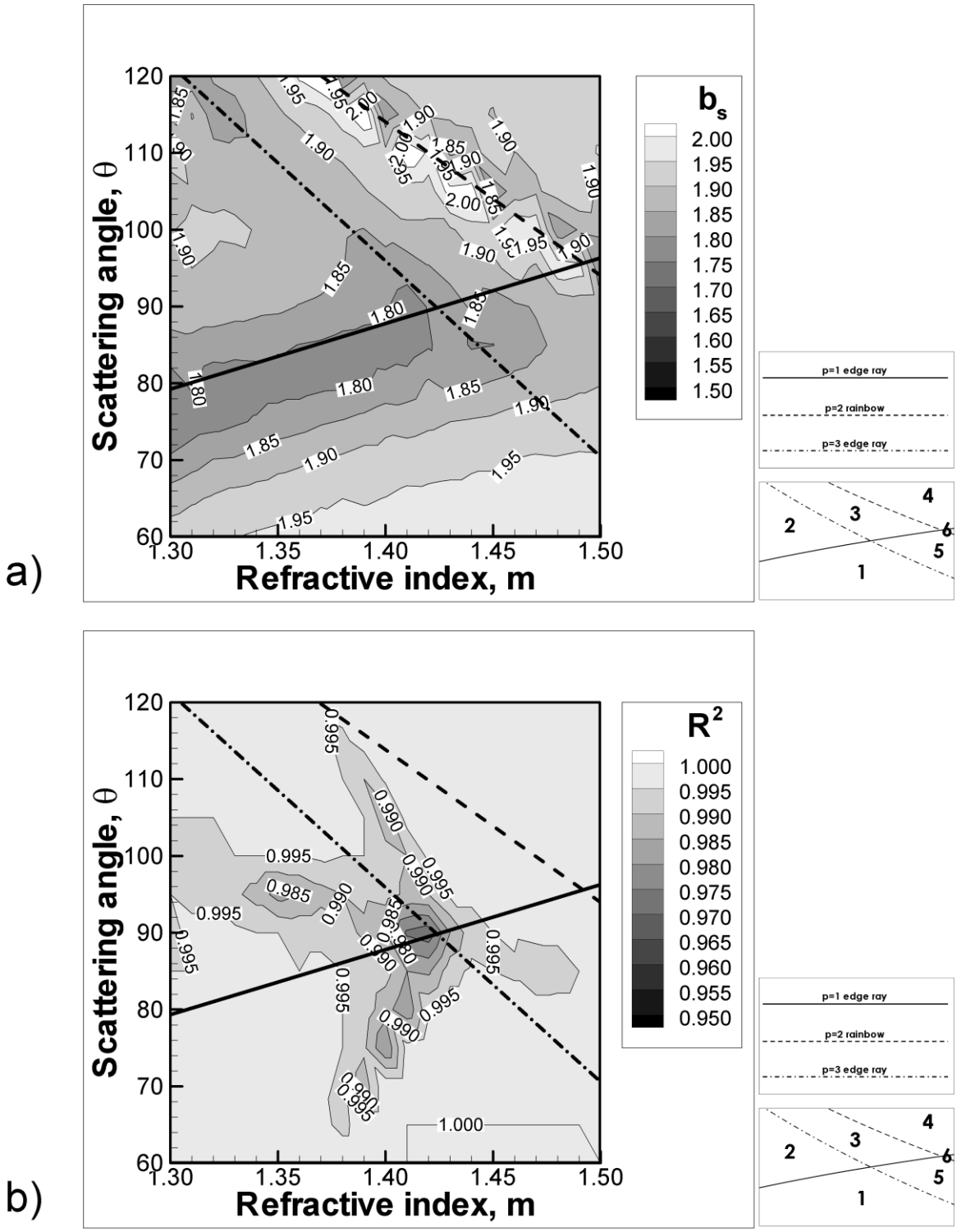

Fig. 8 Contours of a) exponent b_s and b) coefficient of determination R^2 of the power law fit of scattered light intensity, $I_s(D)$, as a function of droplet diameter of eq (7), in the m-θ domain for dye concentration in the liquid c=0.001g/l.

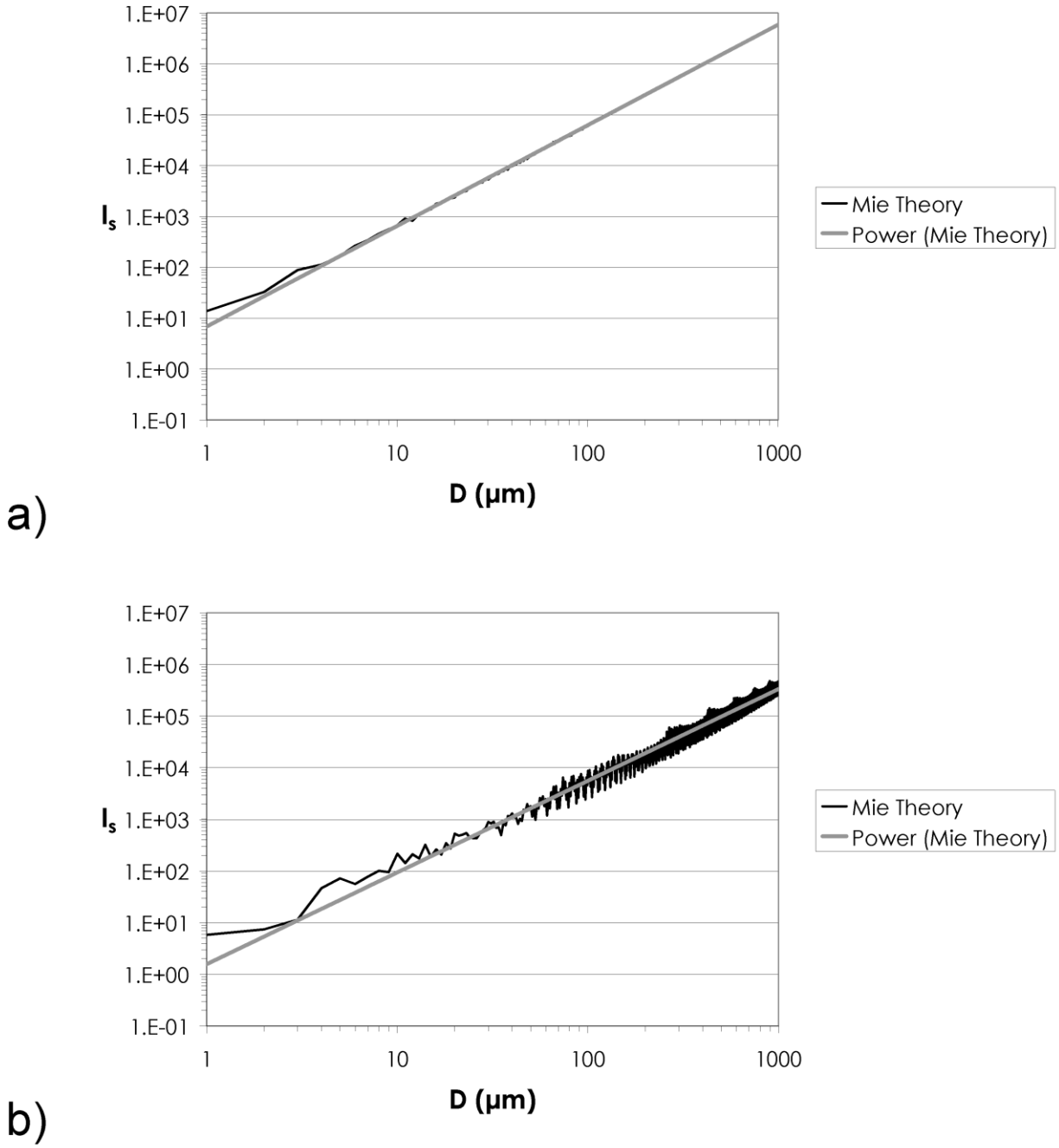

Fig. 9 Dependence of scattered light intensity, $I_s(D)$, on droplet diameter at a) $\theta=60°$ and b) $\theta=90°$ for dye concentration in liquid c=0.001g/l and m=1.41. The oscillations of $I_s(D)$ at $\theta=90°$ are attenuated when light is collected at $\theta=60°$.

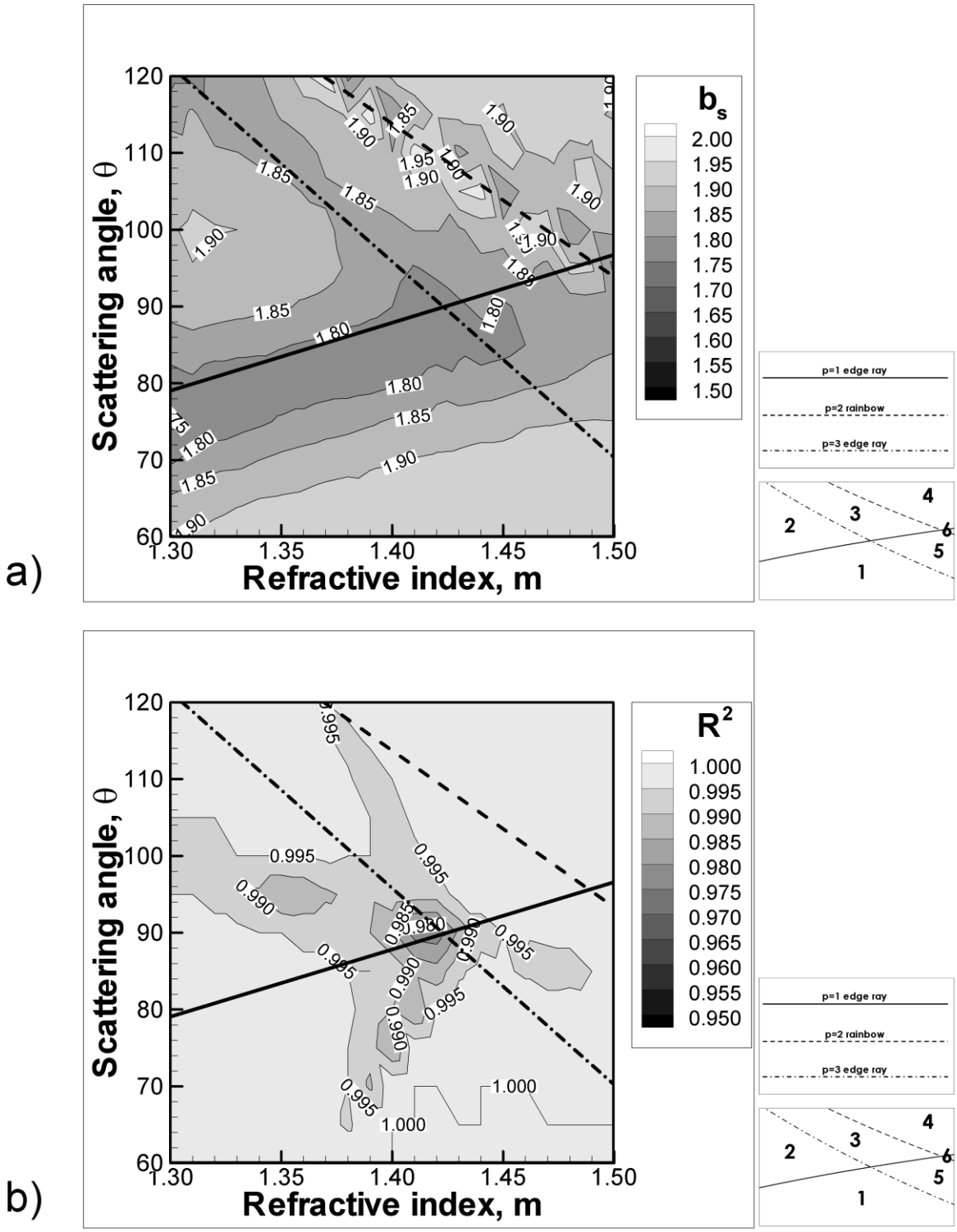

Fig. 10 Contours of a) exponent b_s and b) coefficient of determination R^2 of the power law fit of scattered light intensity, $I_s(D)$, as a function of droplet diameter of eq (7), in the m-θ domain for dye concentration in the liquid c=0.010g/l.

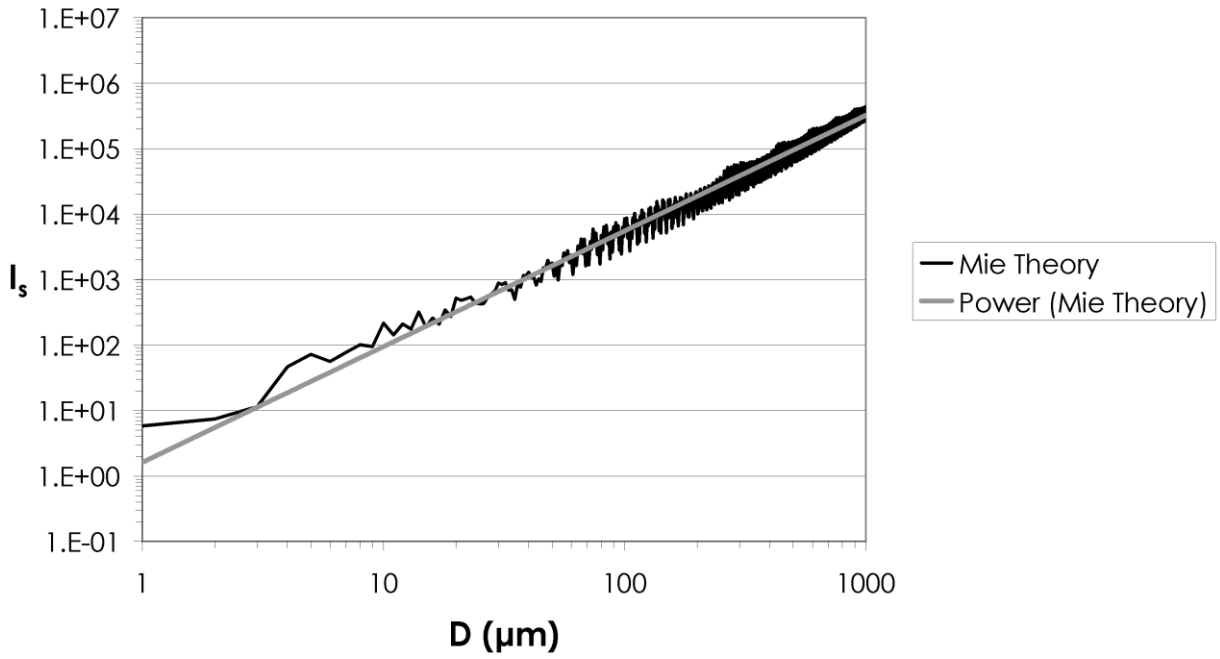

Fig. 11 Dependence of scattered light intensity, $I_s(D)$, on droplet diameter at $\theta=90°$, for dye concentration in the liquid c=0.010g/l and m=1.41. Oscillations of $I_s(D)$ persist at this dye concentration.

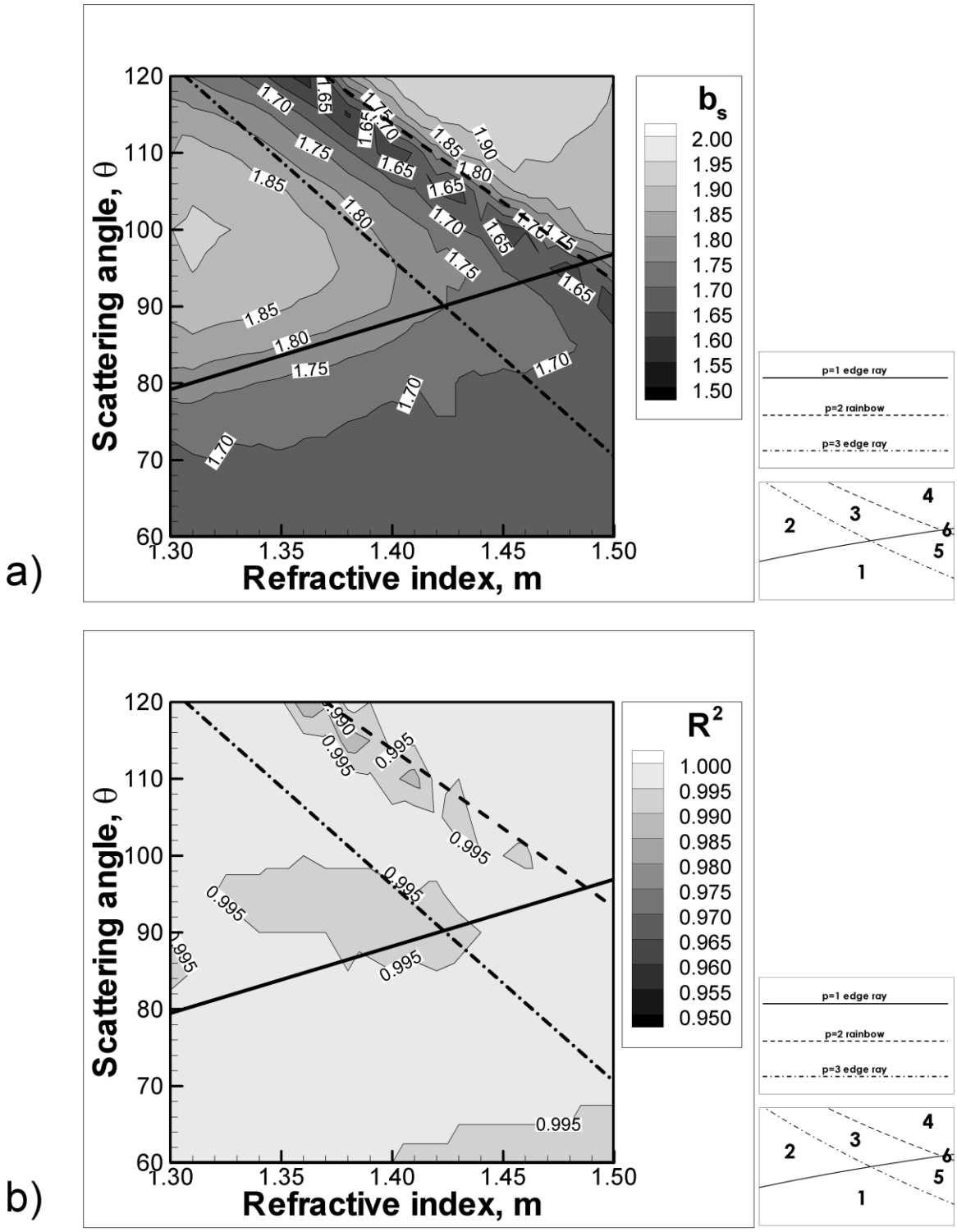

Fig. 12 Contours of a) exponent b_s and b) coefficient of determination R^2 of the power law fit of scattered light intensity, $I_s(D)$, as a function of droplet diameter of eq (7), in the m-θ domain for dye concentration in the liquid c=0.100g/l

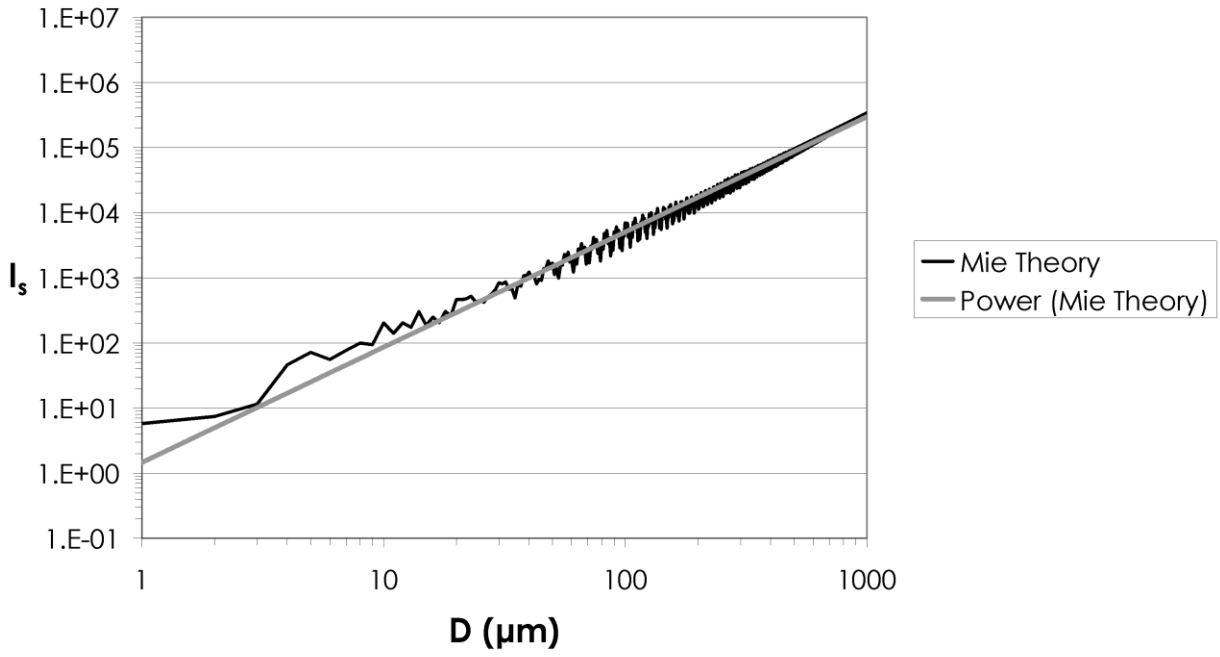

Fig. 13 Profile of $I_s(D)$ at $\theta=90°$ for dye concentration in the liquid c=0.100g/l and m=1.41. Oscillations of $I_s(D)$ are severely attenuated at this dye concentration.

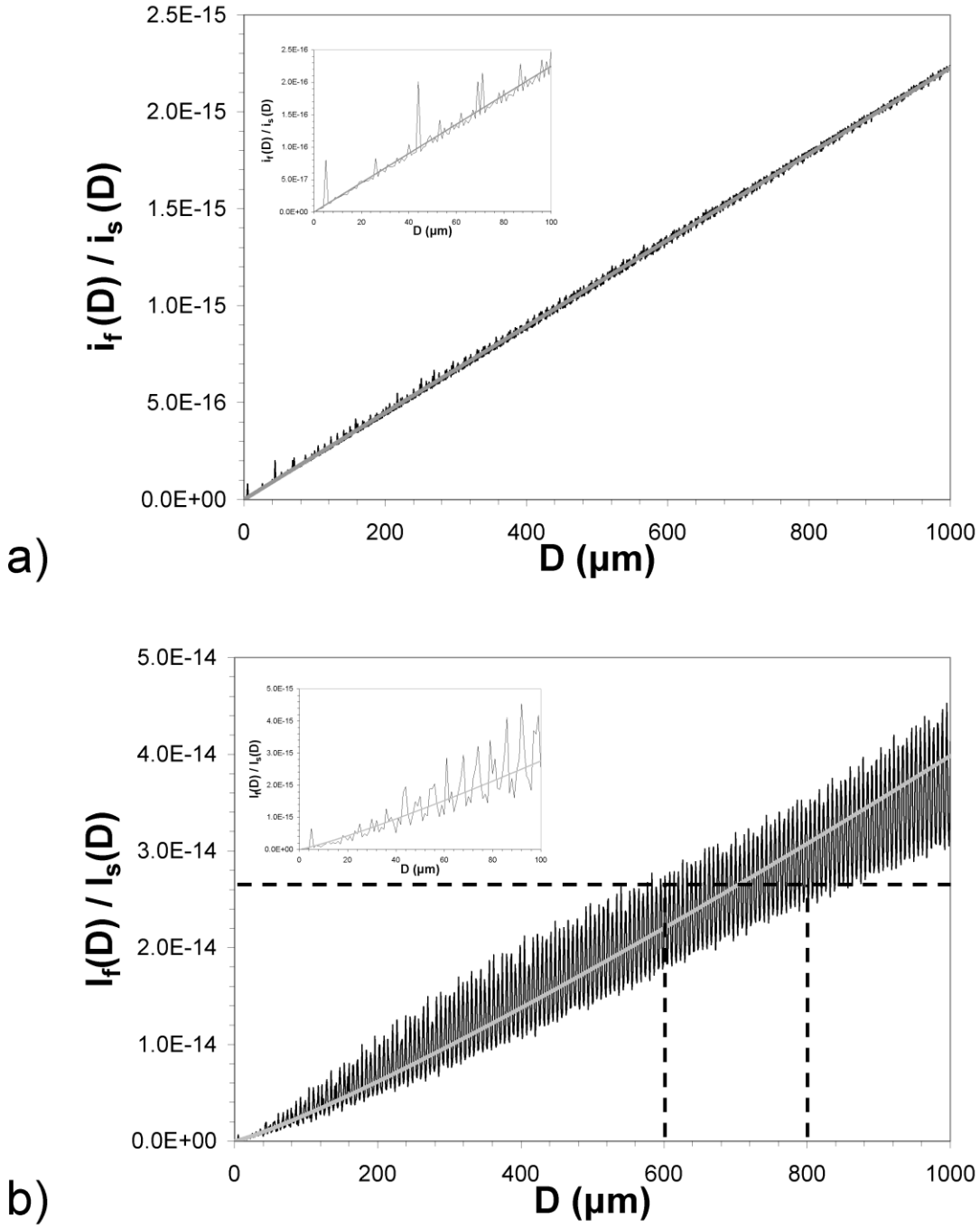

Fig. 14 Profile of the $I_f(D)/I_s(D)$ ratio for dye concentration in the liquid c=0.001g/l and m=1.40. At a) θ=60°, there is a linear dependence of $I_f(D)/I_s(D)$ to droplet diameter with minimal oscillations of $I_f(D)/I_s(D)$. At b) θ=90°, there is a non-linear and non-monotonic dependence of $I_f(D)/I_s(D)$ ratio on droplet diameter with large oscillations of $I_f(D)/I_s(D)$.